Quasi-two-dimensional turbulence in shallow fluid layers: The role of bottom friction and fluid layer depth

H. J. H. Clercx, G. J. F. van Heijst, and M. L. Zoeteweij
Fluid Dynamics Laboratory, Department of Physics, Eindhoven University of Technology, P.O. Box 513, 5600 MB Eindhoven, The Netherlands

(Received 19 December 2002; published 13 June 2003)

The role of bottom friction and the fluid layer depth in numerical simulations and experiments of freely decaying quasi-two-dimensional turbulence in shallow fluid layers has been investigated. In particular, the power-law behavior of the compensated kinetic energy $E_0(t)=E(t)e^{2\lambda t}$, with $E(t)$ the total kinetic energy of the flow and λ the bottom-drag coefficient, and the compensated enstrophy $\Omega_0(t)=\Omega(t)e^{2\lambda t}$, with $\Omega(t)$ the total enstrophy of the flow, have been studied. We also report on the scaling exponents of the ratio $\Omega(t)/E(t)$, which is considered as a measure of the characteristic length scale in the flow, for different values of λ. The numerical simulations on square bounded domains with no-slip boundaries revealed bottom-friction independent power-law exponents for $E_0(t)$, $\Omega_0(t)$, and $\Omega(t)/E(t)$. By applying a discrete wavelet packet transform technique to the numerical data, we have been able to compute the power-law exponents of the average number density of vortices $\rho(t)$, the average vortex radius $a(t)$, the mean vortex separation $r(t)$, and the averaged normalized vorticity extremum $\omega_{ext}(t)/\sqrt{E(t)}$. These decay exponents proved to be independent of the bottom friction as well. In the experiments we have varied the fluid layer depth, and it was found that the decay exponents of $E_0(t)$, $\Omega_0(t)$, $\Omega(t)/E(t)$, and $\omega_{ext}(t)/\sqrt{E(t)}$ are virtually independent of the fluid layer depth. The experimental data for $\rho(t)$ and $a(t)$ are less conclusive; power-law exponents obtained for small fluid layer depths agree with those from previously reported experiments, but significantly larger power-law exponents are found for experiments with larger fluid layer depths.

DOI: 10.1103/PhysRevE.67.066303 PACS number(s): 47.32.Cc, 47.27.Eq

I. INTRODUCTION

During the last decade, several experimental studies were reported on the behavior of quasi-two-dimensional flows in electromagnetically forced shallow fluid layers [1–7]. In many of these experiments, it is assumed that the two-dimensionality (2D) hypothesis for such flows holds (see Refs. [1,3–6]), and that bottom friction can be accounted for with the relatively simple Rayleigh friction model. The validity of these assumptions has been investigated numerically by Satijn *et al.* [8] for an evolving axisymmetric monopolar vortex in a shallow fluid layer. For the more complex case of decaying quasi-2D turbulence, Paret *et al.* [9] claimed, based on experimental measurement of relaxation times for decaying monopolar and dipolar structures (in thin density-stratified fluid layers), that the flow could indeed be considered as two-dimensional after a short initial transient state (where the flow is dominated by three-dimensional residual flows). A numerical study of decaying 2D turbulence (with stress-free boundaries) by Jüttner *et al.* [10] yielded similar conclusions. Although these studies (Refs. [8–10]) provided important insights, any extrapolation to decaying quasi-2D turbulence in shallow fluid layers is in our opinion premature due to the far more complex flow behavior. It was therefore felt necessary to investigate the influence of the bottom friction and the fluid layer depth on decaying quasi-2D turbulence in more detail.

We proceed from two different starting points. With numerical simulations of decaying 2D turbulence on a bounded square domain with Rayleigh damping, which represents the bottom friction, we have investigated the power-law exponents of both the compensated kinetic energy $E_0(t)=E(t)e^{2\lambda t}$, with $E(t)$ the total kinetic energy of the flow and λ the bottom-drag coefficient, and the compensated enstrophy $\Omega_0(t)=\Omega(t)e^{2\lambda t}$, with $\Omega(t)$ the total enstrophy of the flow. The decay exponent of the ratio $\Omega(t)/E(t)$, representing an estimate of the characteristic length scale in the flow, has also been computed, and the temporal evolution of coherent vortices in decaying 2D turbulence with bottom friction has been investigated. An important aspect is the numerical validation of the so-called compensated vorticity and velocity fields as proposed by Hansen *et al.* [6]. Additionally, the influence of the fluid depth has been investigated by measuring $E_0(t)$, $\Omega_0(t)$, $\Omega(t)/E(t)$, and the temporal evolution of the vortices in a series of experiments.

In Sec. II, we summarize the theory of flows in shallow fluid layers. Subsequently, we will discuss the power-law exponents obtained from direct numerical simulations (DNS) in Sec. III. The experimental data are presented in Sec. IV. We will conclude in Sec. V with a short discussion of the results.

II. THEORY OF 2D TURBULENCE IN SHALLOW FLUID LAYERS

The effect of bottom friction is usually parametrized by a linear friction term $-\lambda\mathbf{v}$ in the 2D Navier Stokes equation, with λ the so-called bottom-drag coefficient. Cartesian coordinates in a frame of reference are denoted by x and y, and $\mathbf{v}=(u,v)$ represents the horizontal fluid velocity in the shallow fluid layer. The bottom-drag coefficient can be expressed in terms of the kinematic viscosity ν and the fluid layer depth H: $\lambda=\nu(\pi/2H)^2$. The dimensionless 2D Navier-Stokes equation takes the following form:

$$\frac{\partial \mathbf{v}}{\partial t}+(\mathbf{v}\cdot\boldsymbol{\nabla})\mathbf{v}=-\boldsymbol{\nabla}p+\frac{1}{\mathrm{Re}}\nabla^2\mathbf{v}-\frac{1}{\mathrm{Re}_\lambda}\mathbf{v}. \tag{1}$$

The horizontal Reynolds number is defined as $\mathrm{Re}=UL/\nu$, with U and L being characteristic horizontal velocity and length scales of the flow, and represents the usual Reynolds number for purely 2D flows. The vertical Reynolds number is defined as $\mathrm{Re}_\lambda=U/\lambda L$. The parametrization of the bottom friction by $-\lambda\mathbf{v}$ turns out to be adequate for an axisymmetric vortex in a shallow fluid layer with a sufficiently small horizontal and vertical Reynolds number: $\mathrm{Re}\lesssim 2500$ and $\mathrm{Re}_\lambda \lesssim 25$ [8]. Note that the estimates of these dimensionless numbers depend on the somewhat arbitrary choice of the criterion to distinguish between a more or less three-dimensional and a quasi-two-dimensional flow (see Ref. [8] for details).

The relative importance of bottom friction with respect to horizontal diffusion can easily be understood from the ratio $\mathrm{Re}_\lambda/\mathrm{Re}=(2H/\pi L)^2$. Thus, $\mathrm{Re}_\lambda \ll \mathrm{Re}$ for flows in extremely shallow fluids (with $H \ll L$). The dissipative term $1/\mathrm{Re}_\lambda\mathbf{v}$ will generally dominate over lateral diffusion $1/\mathrm{Re}\nabla^2\mathbf{v}$, and the decay of the flow is completely governed by the bottom friction. Choosing the experimental or numerical parameters in this regime, i.e., $H \ll L$, might have severe consequences for decaying 2D turbulent flows, because due to bottom friction any nonlinearity is rapidly depleted and the inverse energy cascade [11] is virtually halted; the flow dynamics will be frozen by bottom friction before the larger structures are able to emerge. The final number of coherent structures might therefore be substantially larger than one when bottom friction is present. In the absence of bottom friction, usually one or two vortices are observed in the quasistationary final state of decaying 2D turbulence [12,13].

The total kinetic energy of the two-dimensional flow is defined as $E=\frac{1}{2}\int_{\mathcal{D}}\mathbf{v}^2 dA$, with dA an infinitesimal area element of the total flow domain $\mathcal{D}$. In a similar way, the total enstrophy of the flow is defined as $\Omega=\frac{1}{2}\int_{\mathcal{D}}\omega^2 dA$, with $\omega=\partial v/\partial x-\partial u/\partial y$ the vertical vorticity of the flow. A relation between the energy decay rate and the enstrophy is easily derived from Eq. (1),

$$\frac{dE(t)}{dt}=-\frac{2}{\mathrm{Re}}\Omega(t)-\frac{2}{\mathrm{Re}_\lambda}E(t). \tag{2}$$

By introducing the following dimensionless expressions for the energy and the enstrophy:

$$E(t)=E_0(t)e^{-2t/\mathrm{Re}_\lambda} \tag{3}$$

$$\Omega(t)=\Omega_0(t)e^{-2t/\mathrm{Re}_\lambda}, \tag{4}$$

with $E_0(t)$ and $\Omega_0(t)$ independent of the bottom friction, Eq. (2) can be rewritten as

$$\frac{dE_0(t)}{dt}=-\frac{2}{\mathrm{Re}}\Omega_0(t). \tag{5}$$

Apparently, $E_0(t)$ and $\Omega_0(t)$ can be considered as an energy and an enstrophy, respectively, of a 2D flow without bottom friction and are therefore denoted as the compensated kinetic energy and the compensated enstrophy of the flow, respectively. Moreover, it indicates that we might introduce the following relations for the velocity and the vorticity: $\mathbf{v}(x,y,t)=\mathbf{v}_0(x,y,t)e^{-t/\mathrm{Re}_\lambda}$ and $\omega(x,y,t)=\omega_0(x,y,t)e^{-t/\mathrm{Re}_\lambda}$. Note that x, y, and t are all dimensionless.

The ratio $\Omega(t)/E(t)$ provides an estimate of the average length scale l in the flow via $\sqrt{\Omega(t)/E(t)}\propto 1/l$. Using Eqs. (3) and (4), we see directly that

$$\frac{\Omega(t)}{E(t)}=\frac{\Omega_0(t)}{E_0(t)}, \tag{6}$$

and l should therefore be independent of the bottom friction.

Although the above analysis suggests independence of $E_0(t)$, $\Omega_0(t)$, and $\Omega(t)/E(t)$ from the bottom friction, and seems to result in a straightforward simplification of the description of decaying 2D turbulence in shallow fluid layers, we would like to emphasize that thorough numerical or experimental justification of this approach is sparse.

Keeping Eqs. (3) and (4) in mind, we can further simplify the 2D Navier-Stokes equation with bottom friction. For this purpose (and also for numerical purposes later on), we introduce the following vorticity equation with bottom friction:

$$\frac{\partial \omega}{\partial t}+(\mathbf{v}\cdot\boldsymbol{\nabla})\omega=\frac{1}{\mathrm{Re}}\nabla^2\omega-\frac{1}{\mathrm{Re}_\lambda}\omega. \tag{7}$$

We now adapt the procedure, introduced by Hansen *et al.* [6], to simplify the vorticity equation. Substitution of $\omega(x,y,t)=\omega_0(x,y,t)e^{-t/\mathrm{Re}_\lambda}$ and $\mathbf{v}(x,y,t)=\mathbf{v}_0(x,y,t)e^{-t/\mathrm{Re}_\lambda}$ in Eq. (7), subsequently multiplying by $e^{t/\mathrm{Re}_\lambda}$, and finally, introducing a new dimensionless time,

$$t_*=\mathrm{Re}_\lambda(1-e^{-t/\mathrm{Re}_\lambda}) \tag{8}$$

(note that $\lim_{\lambda\to 0}t_*=t$, and $t_*\approx t$ if $t\lesssim\mathrm{Re}_\lambda$), we arrive at the following modified vorticity equation:

$$\frac{\partial \omega_0}{\partial t_*}+(\mathbf{v}_0\cdot\boldsymbol{\nabla})\omega_0=\frac{1}{\mathrm{Re}_*}\nabla^2\omega_0. \tag{9}$$

The price to be paid for this transformation is the appearance of a time-dependent Reynolds number $\mathrm{Re}_*=\mathrm{Re}e^{-t/\mathrm{Re}_\lambda}$ (or a time-dependent viscosity $\nu_*=\nu\, e^{t/\mathrm{Re}_\lambda}$).

Summarizing, we can state that the approach introduced by Hansen *et al.* [6] implies that two-dimensional flows with bottom friction can be interpreted as purely 2D flows without bottom friction, but with a time-dependent horizontal Reynolds number, which can evolve for a finite time t_* ($\lesssim\mathrm{Re}_\lambda$) only. The validity and limitations of this approach will be investigated based on a comparison of numerical data from several decaying 2D turbulence runs with different values of the bottom friction.

TABLE I. The number of simulations per combination of Re and Re_λ.

$\mathrm{Re}_\lambda =$	∞	100	50	33.3	25	20	10
Re=1000	4	4	4	2	4	2	2
Re=2000	4	4	4	2	4	2	2
Re=5000	2	1	1	1	1	1	1

III. DNS OF 2D TURBULENCE WITH RAYLEIGH DAMPING

The objective of the numerical part of this study is to show the bottom-friction independence of $E_0(t)$, $\Omega_0(t)$, and $\Omega(t)/E(t)$. Additionally, it will be shown that the temporal evolution of coherent vortices appears to be independent of the bottom friction as well.

The numerical simulations were carried out with a 2D Chebyshev pseudospectral code (for details see Ref. [14]), and the same setup as was used for the vortex statistics study reported by Clercx and Nielsen [15]; an array of 10×10 vortices of approximately equal strength and size. Their positions and strengths were all perturbed slightly in order to break the symmetry of the flow. The vorticity distribution is similar to the initial vorticity field in the experiments (see Sec. IV). Obviously, the main difference with the numerical experiments in Ref. [15] is the Rayleigh damping term, which has been included in the presently discussed simulations. The horizontal (integral-scale) Reynolds number $\mathrm{Re}=UW/\nu$, with U the rms velocity of the initial flow field and W the half width of the computational domain, is varied between 1000 and 5000. Time has been made dimensionless by W/U and vorticity by U/W. The initial microscale Reynolds number is defined as (see also Ref. [7]): $\mathrm{Re}_{micr}=2\mathrm{Re}/\omega_0$, with ω_0 the (dimensionless) initial rms vorticity. In our numerical experiments $\omega_0=38.0\pm0.5$, thus corresponding with Re_{micr} between 53 and 263. This range of microscale Reynolds numbers is comparable with the Reynolds numbers in the experiments by Danilov *et al.* [7]. Several values of the vertical Reynolds number Re_λ (10, 20, 25, 33.3, 50, 100, and ∞) have been used. We display our data as functions of the dimensionless time τ, which is defined as $\tau=\omega_0 t/N\approx4t$, with t the dimensionless time and N^2 the number of vortices initially present ($N=10$ in the present simulations). The characteristic (initial) dimensionless eddy turnover time is then represented by $\tau\approx1$.

As a first step, we have carried out a series of simulations to investigate the bottom-friction independence of the ratio $\Omega(\tau)/E(\tau)$. Basically, the data represent averages of runs with similar initial conditions (see Ref. [15]), except for Re $=5000$ due to limited computer resources (for an overview of the runs, see Table I). In Fig. 1, a log-log plot of the evolution of $\Omega(\tau)/E(\tau)$ is shown for simulations with Re $=1000$, 2000, and 5000. The algebraic decay rate is found to be independent of the bottom friction up to $\tau\approx50$: $\Omega(\tau)/E(\tau)\propto\tau^{-\alpha}$ with $\alpha=1.15\pm0.10,1.00\pm0.10$, and 0.80 ± 0.10 for Re$=1000$ (a), 2000 (b), and 5000 (c), respectively. Beyond $\tau\approx50$, any relation between the different curves seems nonexistent. Approximately 10% of the initial kinetic energy of the flow is left for the runs without bottom friction, and even less for the runs with bottom friction. Therefore, we might assume that the flow evolution is largely dominated by lateral diffusion for $\tau\gtrsim50$. Nevertheless, it is possible to assign an estimate of the decay rate: $\alpha=0.6\pm0.1$.

In Fig. 2, a log-log plot of the evolution of $\Omega(\tau_*)/E(\tau_*)$ is shown for simulations with Re$=1000$ (a), 2000 (b), and 5000 (c). (Note that $\tau_*\approx4t_*$.) The curves shown in Figs. 2(a)–2(c) reveal that $\Omega(\tau_*)/E(\tau_*)$ and the associated decay exponents become heavily dependent on the bottom friction for $\tau\gtrsim50$. Note that $\tau\approx\tau_*$ for $\tau\lesssim4\mathrm{Re}_\lambda$, thus similar power-law exponents should be found in this regime for $\Omega(\tau)/E(\tau)$ and $\Omega(\tau_*)/E(\tau_*)$. These data support our impression that application of the rescaling introduced by Hansen *et al.* [6] [see Eq. (9)] also does not provide additional information for $\tau\gtrsim50$. In this regime, lateral diffusion is dominating the flow evolution, and in our opinion no power-law behavior should be assigned to the numerical data.

The compensated enstrophy $\Omega_0(\tau)\propto\tau^{-\beta}$ is shown in Fig. 3 for Re$=1000$ (a), 2000 (b), and 5000 (c). These plots clearly show the bottom-friction independence of the compensated enstrophy. The power-law exponents obtained from the present runs are $\beta=1.60\pm0.10$, 1.35 ± 0.10, and 1.05 ± 0.10, respectively. Applying the rescaling proposed by Hansen *et al.* [6] again introduces different curves (for sufficiently large τ_*) for different values of Re_λ [see Fig. 4

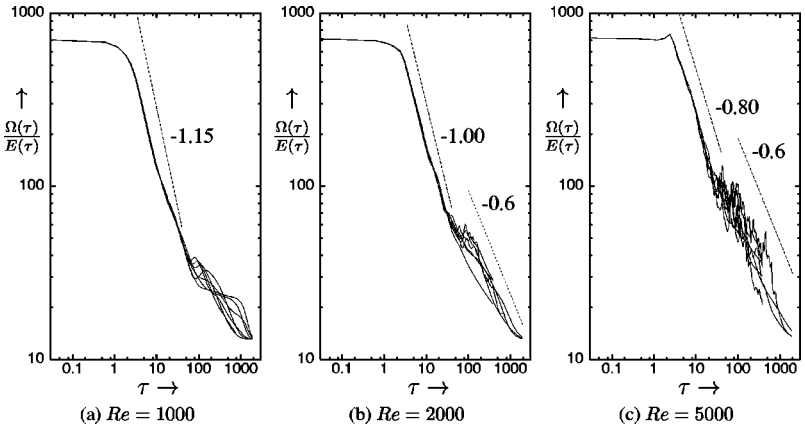

FIG. 1. Time evolution of the ratio $\Omega(\tau)/E(\tau)$ for Re$=1000$ (a), Re$=2000$ (b), and Re$=5000$ (c). $\mathrm{Re}_\lambda\in\{10,20,25,33.3,50,100,\infty\}$.

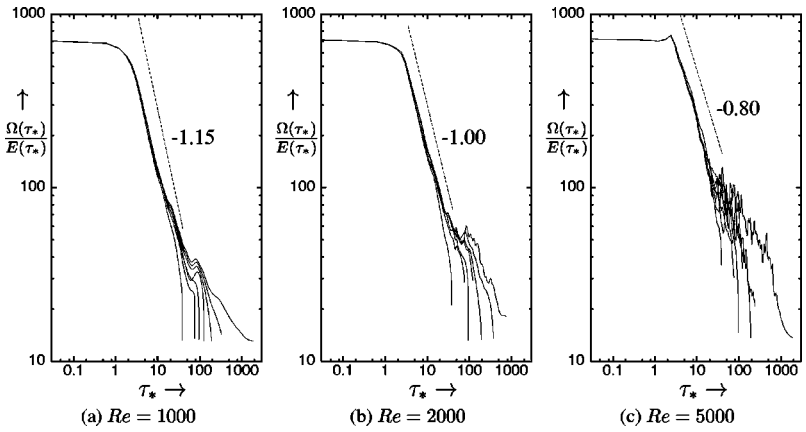

FIG. 2. Time evolution of the ratio $\Omega(\tau_*)/E(\tau_*)$ for Re=1000 (a), Re=2000 (b), and Re=5000 (c). $\mathrm{Re}_\lambda \in \{10,20,25,33.3, 50,100,\infty\}$.

where we have plotted $\Omega_0(\tau_*)$ for Re=5000].

Similar conclusions can be drawn for the decay rate of the compensated energy $E_0(\tau)$ and for the decay rate of the compensated palinstrophy $P_0(\tau)$ [the palinstrophy is a measure of the vorticity gradients in the flow: $P = \frac{1}{2}\int_{\mathcal{D}}(\nabla\omega)^2 dA$]. The power-law exponents are summarized in Table II for different values of the Reynolds number together with the results of the simulations by Clercx and Nielsen [15] (DNS of decaying 2D turbulence without bottom friction with Re=5000, 10 000, and 20 000). The decay rates proved to be independent of the bottom-drag coefficient λ.

The computation of the average number density of vortices $\rho(\tau)$, the average vortex radius $a(\tau)$, the mean vortex separation $r(\tau)$, and the averaged normalized extreme vorticity value $\omega_{ext}(\tau)/\sqrt{E(\tau)}$ is based on a discrete wavelet packet transform (WPT) technique [16–18]. In order to consider a structure as a vortex, the following conditions should be satisfied. The aspect ratio of the long and short ares of the (nearly) ellipsoidal patch should be smaller than ≈ 2. The (absolute) value of the vorticity extremum should always be larger than 20% of the absolute value of the vorticity extremum of the strongest vortex. The computation of the vortex strength and the vortex radius is performed by taking into account the 20% of the strongest vortices detected by the WPT algorithm only [except in the final stage when the number of vortices becomes too small, i.e., $\rho(\tau) \lesssim 10$]. We have applied the WPT technique to the vorticity data obtained from the runs with Re=2000 and 5000. The average number density of vortices is shown in Fig. 5, and the averaged normalized extreme vorticity value is shown in Fig. 6. Although considerable spreading of the data occurs (especially for Re =5000 where only one run for each finite value of Re_λ was available), power-law behavior could be observed which is largely independent of the bottom friction.

For both Re=2000 and Re=5000, two different power-law regimes can be identified for $\rho(\tau)$. The simulations with Re=2000 revealed that $\rho(\tau) \propto \tau^{-1.1}$ for $\tau \lesssim 50$ and $\rho(\tau) \propto \tau^{-0.5}$ for $\tau \gtrsim 50$ [see Fig. 5(a)]. The data obtained for the runs with Re=5000 revealed: $\rho(\tau) \propto \tau^{-0.8}$ for $\tau \lesssim 60$ and $\rho(\tau) \propto \tau^{-0.5}$ for $\tau \gtrsim 60$ [see Fig. 5(b)]. Applying the rescaling proposed by Hansen *et al.* [6], it appears that the first power-law regime remains largely unaffected. The second power-law regime disappears and the curves become strongly bottom-friction dependent [see Figs. 5(c) and 5(d)]. As observed before for the compensated energy and enstrophy, no additional information is gained by applying the rescaled time τ_* (Eq. 8) to the vortex density.

The averaged normalized extreme vorticity value $\omega_{ext}(\tau)/\sqrt{E(\tau)} \propto \tau^{-\beta}$ with $\beta = 0.45 \pm 0.10$ for Re=2000 [when $\tau \lesssim 60$, but less steep for $\tau \gtrsim 60$ with $\beta \approx 0.27$, see Fig. 6(a)] and $\beta = 0.35 \pm 0.05$ for Re=5000 [for $\tau \lesssim 300$, see Fig. 6(b)]. Figure 6(c) shows $\omega_{ext}(\tau_*)/\sqrt{E(\tau_*)}$ for the case Re =5000. The power-law behavior is clearly lost for $\tau \gtrsim 40$. Similar graphs can be made for the average vortex radius $a(\tau)$ and the mean vortex separation $r(\tau)$. These graphs also indicate that the power-law exponents of both $a(\tau)$ and $r(\tau)$ are independent of the bottom friction. In Table III we have

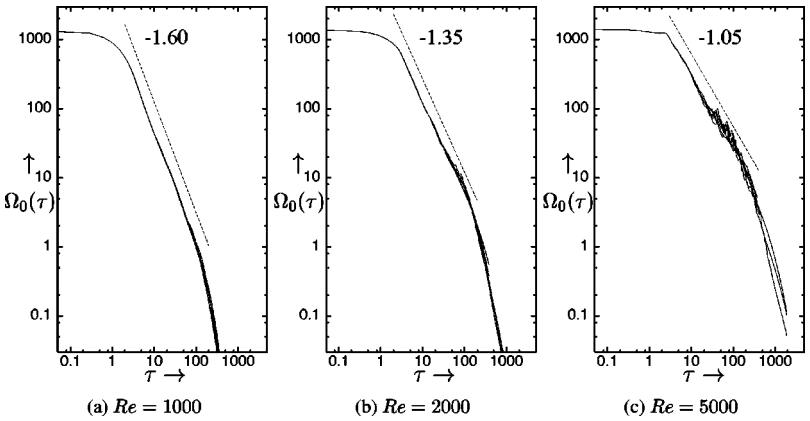

FIG. 3. Time evolution of the compensated enstrophy $\Omega_0(\tau)$ for Re=1000 (a), Re=2000, (b) and Re=5000 (c). $\mathrm{Re}_\lambda \in \{10,20,25,33.3, 50,100,\infty\}$.

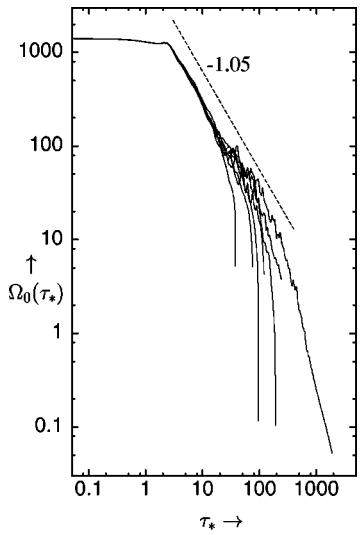

FIG. 4. Time evolution of the compensated enstrophy $\Omega_0(\tau)$ for Re=5000. $\mathrm{Re}_\lambda \in \{10,20,25,33.3,50,100,\infty\}$.

summarized the power-law exponents as obtained from the numerical data in the regime $1 \lesssim \tau \lesssim 50$.

IV. EXPERIMENTS OF QUASI-2D TURBULENCE WITH VARYING FLUID DEPTHS

A. Experimental setup

The experiments were carried out in an electromagnetically forced thin fluid layer in a square plexi-glass container. A similar setup was used before by several investigators, e.g., Dolzhanskii *et al.* [2], Danilov *et al.* [7], and Tabeling and co-workers [1,3–5]. A schematic drawing of the setup is shown in Fig. 7. The dimensions of the container are 52 $\times$52$\times$4 cm (length$\times$width$\times$ height). The container is filled with a solution of salt (NaCl, 12% Brix) up to a certain fluid depth H (varying from 4 to 12 mm in different experiments). Below the black polyvinyl chloride bottom, permanent magnets were placed in a chess-board-like 10$\times$10 pattern (the nearest neighbor distance of the magnets is 5 cm), with alternating poles. The magnets, 25 mm in diameter and 5 mm thick, produce a magnetic field with a maximum of 1.09 T. The magnetic field decays over a typical length of 4 mm. At two facing side-walls, platinum electrodes are positioned in the fluid [see Fig. 7(b)] which are connected to a current supply. In the present experiments, a single current pulse is

TABLE II. Power-law exponents for $E_0(\tau)$, $\Omega_0(\tau)$, $P_0(\tau)$, and $\Omega(\tau)/E(\tau)$ for different integral-scale Reynolds numbers. The power-law exponents for Re=10 000 and 20 000 are from Clercx and Nielsen [12].

Re	$E_0(\tau)$	$\Omega_0(\tau)$	$P_0(\tau)$	$\Omega(\tau)/E(\tau)$
1000	-0.7 ± 0.1	-1.60 ± 0.1	-2.3 ± 0.1	-1.10 ± 0.1
2000	-0.4 ± 0.1	-1.35 ± 0.1	-1.9 ± 0.1	-1.00 ± 0.1
5000	-0.3 ± 0.1	-1.05 ± 0.1	-1.5 ± 0.2	-0.80 ± 0.1
10 000		-0.85 ± 0.1		-0.70 ± 0.1
20 000		-0.80 ± 0.1		-0.65 ± 0.1

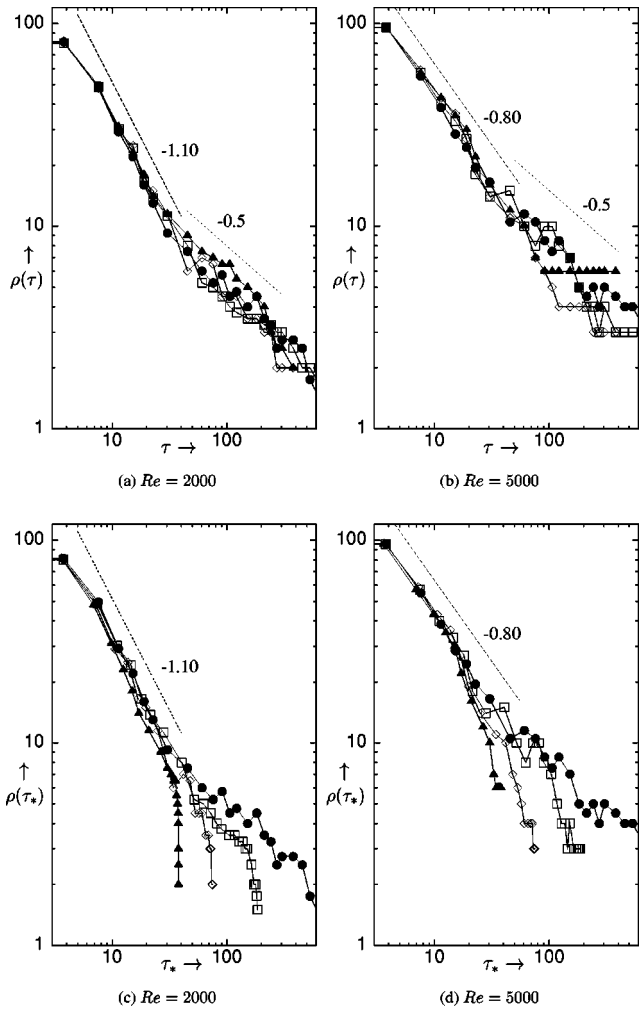

FIG. 5. The time evolution of the average vortex density ρ for Re=2000 (a),(c) and Re=5000 (b),(d). Filled circles, $\mathrm{Re}_\lambda=\infty$; open squares, $\mathrm{Re}_\lambda=50$; open diamonds, $\mathrm{Re}_\lambda=20$; filled triangles, $\mathrm{Re}_\lambda=10$.

chosen, which can be set in amplitude I_f(A) and duration $\Delta\tau_f$(s). Typical values are $I_f=2$ A and $\Delta\tau_f=5$ s.

By putting a potential over the electrodes, a current density $J[\mathrm{A/m}^2]$ will flow through the fluid. This current density J is proportional to the ion concentration n, the charge of the ions q, and the velocity of the ions v_i. The current I_f equals the current density J times the area of the plane perpendicular to the direction of the current. For the total current, this implies that $I_f=JA_\perp=nqv_iHL$, with H and L the fluid depth and the width of the current conducting fluid layer, respectively. With a fixed current I_f, the ion velocity v_i will be inversely proportional to the fluid depth H, and as a consequence the Lorentz force $\mathbf{F}_L=q\mathbf{v}_d\times\mathbf{B}$, with $\mathbf{v}_d$ the drift velocity of the ions and $\mathbf{B}$ the magnetic field vector, will also scale as H^{-1}. For the initial (horizontal) Reynolds number and the energy of the flow, this gives $\mathrm{Re}\sim U\sim 1/H$ and $E\sim U^2\sim 1/H^2$. In order to compare experiments for different fluid depths easily, the velocity should be chosen such that the Reynolds number and energy are comparable for all experiments. To achieve this, the current I_f should scale linearly with the fluid depth H.

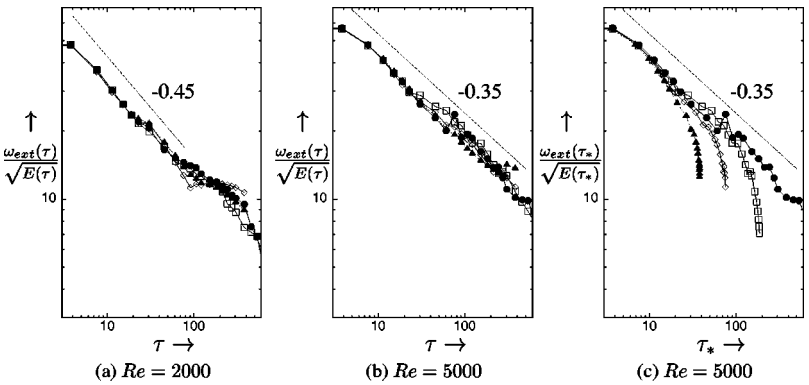

FIG. 6. Time evolution of the ratio $\omega_{ext}(\tau)/\sqrt{E(\tau)}$ for Re=2000 (a) and Re=5000 (b), and of the ratio $\omega_{ext}(\tau_*)/\sqrt{E(\tau_*)}$ for Re =5000 (c). Filled circles, $\mathrm{Re}_\lambda=\infty$; open squares, $\mathrm{Re}_\lambda=50$; open diamonds, $\mathrm{Re}_\lambda=20$; filled triangles, $\mathrm{Re}_\lambda=10$.

For flow visualization and the measurement of several flow quantities, such as the kinetic energy E and the enstrophy Ω, small white tracer particles of 250 μm in size were seeded on the free surface of the fluid layer. The relatively large size and the shape of the tracer particles will result in slightly nonideal behavior. In particular, the particles do not follow the flow exactly. However, the error associated with the nonideal behavior falls within the accuracy of the computation of the velocity vectors. The experiments were recorded with a high-resolution digital gray-level camera at a frame rate of 30 Hz. The flow was illuminated with a xenon lamp or with a laser (QuantaRay GCR 150, 30 Hz Q-switched Nd:YAG (yttrium aluminum garnet) pulse laser with 200 mJ at 532 nm), in order to make the particles clearly visible for the camera. The images taken by the camera were used for high-resolution particle velocimetry calculations [19], which determine the positions and velocities of the particles in the recorded images.

The experimental parameters H, λ, the integral-scale Reynolds number $\mathrm{Re}=UL/\nu$, and the microscale Reynolds number Re_{micr} have been summarized in Table IV. The latter Reynolds number is defined as $\mathrm{Re}_{micr}=2\mathrm{Re}/\omega_{max}(t=0)$, with $\omega_{max}(t=0)$ the peak vorticity of the vortices in the initial flow field at the moment the forcing stopped ($t=0$). Note that the microscale Reynolds number for the experiments is defined in a slightly different way compared with the definition used for the numerical simulations, which is based on the initial (dimensionless) rms vorticity ω_0. However, $\omega_{max}(t=0)$ is of the same order as the initial rms vorticity.

B. Temporal scaling of the energy, the enstrophy, and the vortex density

Several experiments with a very shallow fluid layer have been conducted, and we have indeed observed the exponential decay of the total kinetic energy of the flow. In Fig. 8, the kinetic energy, normalized with the energy $E(t=0)$ (just after forcing), obtained from an experiment with $H=4$ mm is plotted as a function of time. The estimated slope provided the following value for the bottom-drag coefficient: $\lambda=0.14\pm0.02\ \mathrm{s}^{-1}$. This value is in a good agreement with the theoretically predicted Rayleigh friction for a shallow fluid layer with a depth of 4.0 ± 0.2 mm: $\lambda=\pi^2\nu/4H^2=0.16\pm0.02\ \mathrm{s}^{-1}$. In order to compare with a few previously reported measurements (with different fluid depths), it is more convenient to introduce the quantity $\kappa=\lambda H^2/(2\nu)$ [2,7]. The theoretical value is $\kappa=\pi^2/8\approx1.23$ (independent of the fluid depth), and our experimentally obtained value is $\kappa=1.1\pm0.2$. Danilov *et al.* [7] and Dolzhanskii *et al.* [2] conducted similar experiments and found $\kappa=1.7\pm0.2$, considerably larger than found in our experiments.

The compensated kinetic energy, i.e., $E_0(t)=E(t)e^{2\lambda t}$ (see Eq. 3), shows an algebraic decay: $E_0(t)\propto t^{-\alpha}$ with $\alpha>0$. In a similar way, an algebraic expression for the enstrophy decay is found: $\Omega_0(t)\propto t^{-\beta}$ ($\beta>0$). The evolution of the compensated energy and enstrophy is shown in Fig. 9 for an experiment in a shallow fluid layer with a depth of $H=10$ mm. For the energy a power-law exponent of $\alpha=0.45\pm0.05$ fits the experimental data [see Fig. 9(a)]. The enstrophy shows a much larger decay rate, resulting in a power-law exponent $\beta=0.9\pm0.1$ in the range 3 s$\leqslant t\leqslant$20 s [see Fig. 9(b)]. After $t=20$ s, the decay rate decreases slightly. For the same experiment, we have measured the power-law exponent for the ratio $\Omega(t)/E(t)\propto t^{-\gamma}$ and found $\gamma=0.5\pm0.1$.

For several other fluid depths ($H\geqslant8$ mm), similar decay rates have been found for the compensated energy $E_0(t)$ and enstrophy $\Omega_0(t)$. For the experiments with fluid depths of 4 and 6 mm, both $E_0(t)$ and $\Omega_0(t)$ could not be fitted with an algebraic power law with sufficient accuracy. The uncertainty in the measured fluid depth resulted in several possible exponential correction functions, which gave completely dif-

TABLE III. Power-law exponents for $\rho(\tau)$, $a(\tau)$, $r(\tau)$, and $\omega_{ext}(\tau)/\sqrt{E(\tau)}$ for different integral-scale Reynolds numbers ($1\leqslant\tau\leqslant50$). The power-law exponents for Re=10 000 are taken from Clercx and Nielsen [12].

Re	$\rho(\tau)$	$a(\tau)$	$r(\tau)$	$w_{ext}(\tau)/\sqrt{E(\tau)}$
2000	-1.10 ± 0.1	0.35 ± 0.05	0.55 ± 0.1	-0.45 ± 0.05
5000	-0.80 ± 0.1	0.27 ± 0.05	0.45 ± 0.1	-0.35 ± 0.05
10 000	-0.75 ± 0.1	0.25 ± 0.05	0.40 ± 0.1	-0.30 ± 0.05

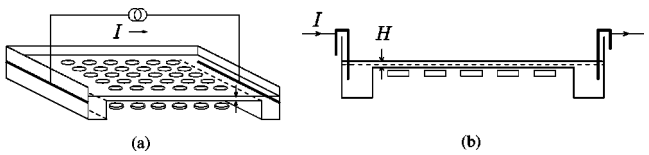

FIG. 7. Schematic representation (a) and cross section (b) of the experimental setup.

TABLE IV. Summary of the experimental parameters H (the fluid depth), λ (the bottom friction), Re (the integral-scale Reynolds number), and Re_{micr} (the microscale Reynolds number).

H (mm)	λ (s^{-1})	Re	Re_{micr}
4	0.15	1500	750
6	0.07	2000	570
8	0.038	3000	1000
10	0.025	2250	1500
12	0.017	2750	920

ferent slopes in the algebraic fits. The power-law exponents for $E_0(t)$, $\Omega_0(t)$, and $\Omega(t)/E(t)$, found in different experiments with $H \geqslant 8$ mm [and $H \geqslant 6$ mm for $\Omega(t)/E(t)$], are summarized in Table V. For this range of fluid layer depths, we could clearly separate the power-law dependence from the exponential decay due to bottom friction. The calculated power-law exponents are based on one experiment for each fluid layer depth, except for $H=10$ mm where they represent an average over data from two experiments. The power-law exponents in Table V seem to be approximately independent of the fluid layer depth.

It is remarkable that the experimentally obtained power-law exponents, and to a lesser extent those obtained from the numerical simulations, do not satisfy Eq. (5). It is clear from Table V that $\beta \neq \alpha+1$ and $\gamma \neq 1$ as one would expect from Eq. (5). The numerically obtained power-law exponents for $E_0(\tau)$, $\Omega_0(\tau)$, and $\Omega(\tau)/E(\tau)$ (see Table II) disagree with the relations $\beta=\alpha+1$ and $\gamma=1$ for the runs conducted with high Reynolds number. This phenomenon has been observed in previous studies and has been addressed numerically by Chasnov [20] for decaying homogeneous 2D turbulence (without bottom friction and with periodic boundary conditions). It has been suggested by Chasnov that the discrepancy might be related with the absence of a pure power law for the decay of the kinetic energy and the enstrophy of the flow.

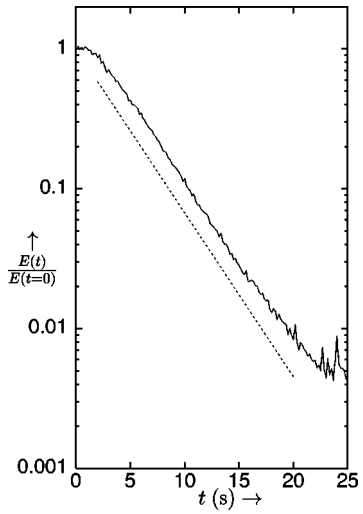

FIG. 8. Decay of the total kinetic energy for a fluid layer of 4 mm. The dashed line indicates the exponential behavior with a fitted value of $\lambda = 0.14\ s^{-1}$.

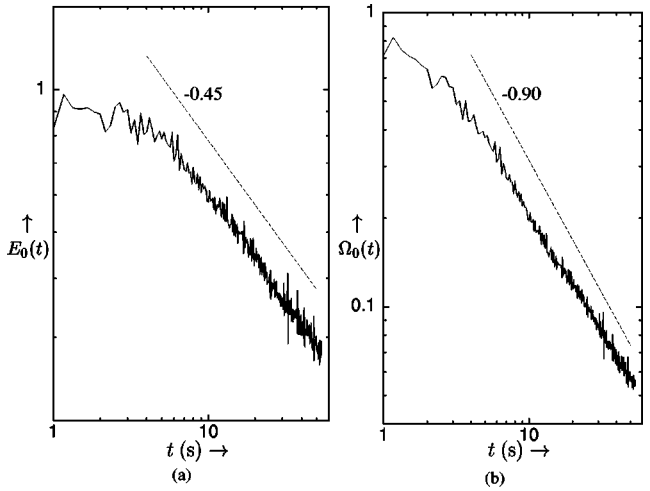

FIG. 9. Evolution of the compensated kinetic energy $E_0(t)$ (a) and the compensated enstrophy $\Omega_0(t)$ (b) calculated from experimental data ($H=10$ mm).

The larger discrepancy between the experimentally obtained values of α, β, and γ is most likely attributed to the additional three-dimensional effects.

Our experimental data on the decay exponent of the compensated enstrophy seem to differ slightly with those reported by Danilov *et al.* [7]. They found different power-law exponents depending on the applied currents to initialize the flow, and the power-law behavior found by them is $\Omega_0(t) \propto t^{-0.8}$. However, their quasi-2D turbulence experiments were conducted in fluid layers with a depth varying from 2 mm to 6 mm (and different horizontal dimensions). Our data suggest a trend to smaller power-law exponents for small fluid layer depths, but we were not able to obtain reliable decay exponents for $H \leqslant 6$ mm. For $H \geqslant 8$ mm, our experimentally measured power-law exponents are somewhat smaller than the predictions by Bartello and Warn ($\beta=1.2$) [21] and by Chasnov ($\beta \approx 1.2$ for the relevant range of Reynolds numbers) [20].

The temporal evolution of coherent vortices could only be determined for flows in fluid layers with $H \geqslant 6$ mm [see Fig. 10, where we have displayed $\rho(t)$ and $a(t)$ for $H=10$ mm and $H=12$ mm]. Unfortunately, no reliable power-law exponents could be determined for $H=4$ mm. The experimentally obtained average number density of vortices, the average vortex radius, and the normalized extremum vorticity show the following algebraic decay behavior for H

TABLE V. Overview of the power-law exponents a, β, and γ for $E_0(t) \propto t^{-a}$, $\Omega_0(t) \propto t^{-\beta}$, and $\Omega(t)/E(t) \propto t^{-\gamma}$, respectively, obtained from experiments with varying fluid layer depth H (in mm).

H	$E_0(t)$ α	$\Omega_0(t)$ β	$\Omega(t)/E(t)$ γ
6			0.4 ± 0.1
8	0.5 ± 0.1	0.9 ± 0.1	0.5 ± 0.1
10	0.5 ± 0.1	0.9 ± 0.1	0.5 ± 0.1
12	0.4 ± 0.1	1.0 ± 0.1	0.5 ± 0.1

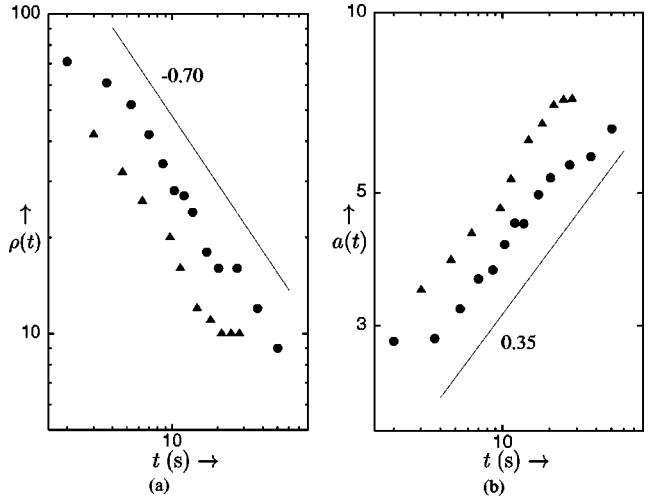

FIG. 10. The time evolution of the average vortex density $\rho(t)$ (a) and the average vortex radius $a(t)$ (b) for experiments with fluid layer thickness $H=10$ mm (filled circles) and $H=12$ mm (filled triangles). The offset between the data obtained for $H=10$ mm and $H=12$ mm is most likely due to the higher microscale Reynolds number for $H=10$ mm (see Table IV).

$\leqslant 8$ mm: $\rho(t)\propto t^{-0.45\pm0.1}$, $a(t)\propto t^{0.17\pm0.05}$, and $\omega_{ext}(t)/\sqrt{E(t)}\propto t^{-0.21\pm0.05}$ for $t\gtrsim 3$ s. These experimental power laws are in a close agreement with the data from similar experiments reported by Cardoso *et al.* [3]; they found $\rho(t)\propto t^{-0.44\pm0.1}$, $a(t)\propto t^{0.22\pm0.03}$, and $\omega_{ext}(t)/\sqrt{E(t)}\propto t^{-0.22\pm0.06}$. For experiments in fluid layers with thickness $H\geqslant 10$ mm, we have found $\rho(t)\propto t^{-0.7\pm0.1}$, $a(t)\propto t^{0.35\pm0.05}$, and $\omega_{ext}(t)/\sqrt{E(t)}\propto t^{-0.22\pm0.05}$ (see Fig. 10). In particular, the absolute value of the decay exponent for $\rho(t)$ and $a(t)$ is significantly larger than those reported for smaller fluid layer depths.

Despite some dependence on the fluid layer depth, particularly for $\rho(t)$ and $a(t)$, the experimental data agree with the numerically computed power-law exponents in the second power-law regime where the flow is already strongly dominated by viscous effects [see Figs. 5 and 6 for $\rho(\tau)$ and $\omega_{ext}(\tau)/\sqrt{E(\tau)}$, respectively]. The initial-stage power laws as found in the simulations might not be captured in the experiments. This is most likely due to the faster dissipation of kinetic energy of the flow in the experiments, due to a combination of bottom friction and three-dimensional residual flows, and will result in a smaller effective horizontal Reynolds number.

V. DISCUSSION AND CONCLUSION

The numerical and experimental studies of the role of bottom friction and fluid layer depth on decaying quasi-two-dimensional turbulence enable several interesting observations. The numerical simulations showed that the evolution of vortex statistics of decaying 2D turbulence with bottom friction can be described by bottom-friction independent power laws (provided that compensated velocity and vorticity fields are used). The rescaling of time ($\tau\rightarrow\tau_*$) proposed by Hansen *et al.* [6] does not modify power-law exponents for $\tau\lesssim 4\mathrm{Re}_\lambda$ (the same power laws are necessarily found), and for $\tau\gtrsim 4\mathrm{Re}_\lambda$ any clear power-law behavior is absent, even if the rescaled time τ_* is introduced. In the latter regime, the computed data show a strong bottom-friction dependence and are strongly dominated by lateral diffusion. Another indication that lateral diffusion is important in the regime $\tau\gtrsim 4\mathrm{Re}_\lambda$ is the absence of freezing of the flow dynamics in virtually all numerical runs. The freezing of the flow dynamics can be understood when the rescaling procedure by Hansen *et al.* [6] is used. Applying the rescaled time τ_* implies the assumption of a finite decay time available for the flow: $\tau_*\leqslant 4\mathrm{Re}_\lambda$. A major consequence should be the ceasing of the vortex merging process. This has not been observed in the present numerical simulations, except for one run with $\mathrm{Re}=5000$ and $\mathrm{Re}_\lambda=10$. These data show that $\rho(\tau)\approx 6$ and remains fixed for quite a long time, see Fig. 5(b). In our opinion, this means that one cannot distinguish between the effects of lateral diffusion and Rayleigh damping, at least for the range of Reynolds numbers considered in the present numerical study. Summarizing, we conclude that one aspect of the proposed rescaling procedure by Hansen *et al.* [6] is very effective; the introduction of the compensated velocity $\mathbf{v}_0=\mathbf{v}e^{\lambda t}$ and the compensated vorticity $\omega_0=\omega e^{\lambda t}$. The other aspect, the introduction of the rescaled time τ_*, appears to be rather ineffective for the present range of Reynolds numbers.

The experiments showed that the temporal evolution of coherent vortices and the power-law regimes of integral quantities like $\Omega(t)/E(t)$ are relatively unaffected by the fluid layer depth for $H\leqslant 12$ mm, with possibly an exception for $\rho(t)$ and $a(t)$ for $H\geqslant 10$ mm. It should, however, be mentioned that no reliable power-law exponents could be obtained for $H\leqslant 4$ mm. The apparent independence of these quantities from the fluid layer depth indicates that residual three-dimensional flows are relatively unimportant for the dynamics of decaying quasi-2D turbulence in shallow fluid layers. However, it seems to contribute to a faster dissipation and a smaller effective Reynolds number.

Assuming vanishing viscosity, and keeping λ finite (which implies $H\propto\sqrt{\nu}$), Hansen *et al.* [6] argued that decaying 2D turbulence with bottom friction can be described by the Euler equations, viz. $D\omega/Dt_*=0$, with the constraint that only a finite decay time is available for the flow ($t_*\leqslant\mathrm{Re}_\lambda$). Proceeding from this point, the temporal evolution of coherent vortices in decaying 2D turbulence [22,23] could, in principle, be validated experimentally. Tabeling *et al.* [1], Cardoso *et al.* [3], and Hansen *et al.* [6] tried to validate the vortex statistics approach with experiments in shallow fluid layers, but their results seem inconclusive. In our opinion, any attempt to validate the scaling theory of Carnevale *et al.* [22] (a theory applicable to inviscid flows only) with experiments in shallow fluid layers is somewhat ambitious. The range of horizontal Reynolds numbers (based on the average vortex size) accessible in these experiments has an upper bound of ≈ 2500. Increasing the Reynolds number further inevitably induces strong three-dimensional residual flows. Additionally, the present numerical investigation indicated that application of the rescaling as discussed

above requires substantially higher Reynolds numbers (Re $\gg 5000$, see also Ref. [15]).

Although we have been able to show that the numerically obtained power-law exponents are bottom-friction independent, and that the experimentally obtained power-law exponents are independent of the fluid layer thickness, it could also be observed that the numerically and experimentally obtained power-law exponents differ considerably. Moreover, the experimental power-law exponents of $\rho(t)$, $a(t)$, and $\omega_{ext}(t)/\sqrt{E(t)}$, measured in experiments with $H \leqslant 8$ mm, agree remarkably well with those reported by Cardoso *et al.* [3]. The difference between the numerical and experimental data is most likely due to the fact that the initial decay stage observed in the numerical simulations might not be captured in the experiments. This seems to be supported by the power-law exponents found for the second (less steep) power-law regime in the numerical data that are rather close to the experimentally obtained power-law exponents: $\Omega(\tau)/E(\tau) \propto \tau^{-0.6\pm0.1}$, $\rho(\tau) \propto \tau^{-0.5\pm0.1}$, and $\omega_{ext}(\tau)/\sqrt{E(\tau)} \propto \tau^{-0.27\pm0.05}$.

ACKNOWLEDGMENTS

We thank Dr. R.R. Trieling (Eindhoven University of Technology, The Netherlands) for comments on this paper. This work is part of the research program ''2D Turbulence'' of the ''Stichting voor Fundamenteel Onderzoek der Materie (FOM),'' which was financially supported by the ''Nederlandse Organisatie voor Wetenschappelijk Onderzoek (NWO).'' Part of this work was sponsored by the Stichting Nationale Computerfaciliteiten (National Computing Facilities Foundation, NCF) for the use of supercomputer facilities, with financial support from the Nederlandse Organisatie voor Wetenschappelijk Onderzoek (Netherlands Organization for Scientific Research, NWO).

[1] P. Tabeling, S. Burkhart, O. Cardoso, and H. Willaime, Phys. Rev. Lett. **67**, 3772 (1991).
[2] F.V. Dolzhanskii, V.A. Krymov, and D.Yu. Manin, J. Fluid Mech. **241**, 705 (1992).
[3] O. Cardoso, D. Marteau, and P. Tabeling, Phys. Rev. E **49**, 454 (1994).
[4] D. Marteau, O. Cardoso, and P. Tabeling, Phys. Rev. E **51**, 5124 (1995).
[5] J. Paret and P. Tabeling, Phys. Rev. Lett. **79**, 4162 (1997).
[6] A.E. Hansen, D. Marteau, and P. Tabeling, Phys. Rev. E **58**, 7261 (1998).
[7] S. Danilov, F.V. Dolzhanskii, V.A. Dovzhenko, and V.A. Krymov, Phys. Rev. E **65**, 036316 (2002).
[8] M.P. Satijn, A.W. Cense, R. Verzicco, H.J.H. Clercx, and G.J.F. van Heijst, Phys. Fluids **13**, 1932 (2001).
[9] J. Paret, D. Marteau, O. Paireau, and P. Tabeling, Phys. Fluids **9**, 3102 (1997).
[10] B. Jüttner, D. Marteau, P. Tabeling, and A. Thess, Phys. Rev. E **55**, 5479 (1997).
[11] R.H. Kraichnan, Phys. Fluids **10**, 1417 (1967).
[12] H.J.H. Clercx, S.R. Maassen, and G.J.F. van Heijst, Phys. Fluids **11**, 611 (1999).
[13] S. Li and D. Montgomery, Phys. Lett. A **218**, 281 (1996).
[14] H.J.H. Clercx, J. Comput. Phys. **137**, 186 (1997).
[15] H.J.H. Clercx and A.H. Nielsen, Phys. Rev. Lett. **85**, 752 (2000).
[16] M. Farge, E. Goirand, Y. Meyer, F. Pascal, and M.V. Wickerhauser, Fluid Dyn. Res. **10**, 229 (1992).
[17] M.V. Wickerhauser, *Adapted Wavelet Analysis from Theory to Software Algorithms* (Peters, Wellesley, 1994).
[18] A. Siegel and J.B. Weiss, Phys. Fluids **9**, 1988 (1997).
[19] G.A.J. van der Plas, R.N. Kieft, and C.C.M. Rindt, in Proceedings of the Third International Workshop on PIV '99-Santa Barbara (unpublished), pp. 177–182.
[20] J.R. Chasnov, Phys. Fluids **9**, 171 (1997).
[21] P. Bartello and T. Warn, J. Fluid Mech. **326**, 357 (1996).
[22] G.F. Carnevale, J.C. McWilliams, Y. Pomeau, J.B. Weiss, and W.R. Young, Phys. Rev. Lett. **66**, 2735 (1991).
[23] J.B. Weiss and J.C. McWilliams, Phys. Fluids A **5**, 608 (1993).